

Ling Yang
Di An
Ting-Jie Wang*
Chengyou Kan
Yong Jin

Photodegradation of Polymer Materials Used for Film Coatings of Controlled-Release Fertilizers

The photodegradation of three polymer materials was studied, i.e., polyolefin, polyurethane, and a copolymer of styrene, butyl acrylate, and methyl methacrylate (P(St-co-BA-co-MMA) latex). These polymers are mostly used as film-coating materials for producing controlled-release fertilizers. The P(St-co-BA-co-MMA) latex film degraded at the highest rate and the film surface became porous under UV irradiation. The weak cross-link chain in the latex film was broken and the connections between the microspheres were destroyed. A photo-oxidative aging reaction weakened the tenacity of the latex film, which resulted in the easy release of microspheres from the film, leading to a reduction in film thickness and film tensile strength. Therefore, P(St-co-BA-co-MMA) latex is a promising coating material for controlled-release fertilizers.

Keywords: Controlled-release fertilizer, Fertilizer, Film coating, Photodegradation, Polymer latex

Received: February 29, 2016; *revised:* February 13, 2017; *accepted:* April 21, 2017

DOI: 10.1002/ceat.201600120



Supporting Information
available online

1 Introduction

The low efficiency at which plants utilize fertilizers has caused severe environmental pollution. The use of controlled-release fertilizers can increase their efficiency. Synthetic polymers have been employed as coating materials in various processes for the production of controlled-release fertilizers: (1) a polymer is dissolved in organic solvent and taken as the coating material [1–3]; (2) the coating material consists of multiple components that form polymer films with different thermostettings, such as a polyurethane (PU) film and an alkyd resin film [4–6]; and (3) polymer latex with water as the continuous phase is applied as a coating material by spraying the latex onto the surfaces of fertilizer particles to coat them with films after dehydration. This process is free of organic solvents and is considered promising as a green approach to producing controlled-release fertilizers [7–9].

Residual films left in the soil after the nutrient release from the polymer-coated fertilizers is finished, may affect the moisture level, nutrient delivery, and structural properties of the soil, such as permeability [10, 11]. The effect of residual films on soil mainly results from the blocking of the permeation of molecules or ions into the soil. Polyethylene (PE), polypropylene (PP), and PU are currently the main coating materials used for the production of controlled-release fertilizers. The build-up of polymer residues will block the permeation of the molecule or ion into soil. Therefore, the residual film needs to be degraded. Several degradation methods are available, including photodegradation and biodegradation.

Compared with photodegradation, biodegradation is highly dependent on the microbial species and soil environment, and

it is less effective for high-molecular-weight polymers [12]. Moreover, biodegradable materials demand more stringent storage conditions [13, 14]. The photochemical activities of polymers can be increased by the addition of photocatalysts [15–17]. Shang et al. [15] incorporated TiO₂ nanoparticles into polystyrene (PS) plastics and achieved a 22.5% weight loss under 150 h of ultraviolet (UV) light irradiation, whereas without the addition of TiO₂ nanoparticles, the weight loss was only 12.0%. Zhao et al. [18] introduced TiO₂ nanoparticles into PE to form a complex film that showed a high photocatalytic activity under UV light and sunlight.

In the absence of photocatalysts, the photochemical activity of a polymer governs its photodegradation performance. Free radicals are generated in the degradation process, which generally consists of initiation, propagation, and termination [19]. The polymer chain is broken or cross-linked in the free radical transfer process [20, 21]. Photodegradation highly depends on the types and concentrations of light-absorbing chromophores that are present in the polymers [22, 23].

Here, the permeabilities of three types of coating materials for producing controlled-release fertilizers, i.e., polyolefin, PU, and a copolymer of styrene, butyl acrylate, and methyl

Dr. Ling Yang, Dr. Di An, Prof. Ting-Jie Wang, Prof. Chengyou Kan,
Prof. Yong Jin
wangtj@tsinghua.edu.cn
Department of Chemical Engineering, Tsinghua University, Beijing,
100084, China.

methacrylate (P(St-co-BA-co-MMA) latex, were measured. The photodegradation performance of these polymer materials under UV irradiation and the photodegradation mechanism of the P(St-co-BA-co-MMA) latex film were investigated.

2 Experimental

2.1 Materials and Instruments

Xylene (chemically pure, Beijing Chemical Works, China), PE (K7726H, technically pure, SINOPEC Beijing Yanshan Company, China), and PP (1C7A, technically pure, SINOPEC Beijing Yanshan Company, China) were used to prepare the polyolefin films. Diphenyl methane diisocyanate (MDI, technically pure, PM-200, -NCO: 30.2–32.0 wt %, Wanhua Chemical Group Co., Ltd. China), hexamethylene diisocyanate (HDI, technically pure, N3390, -NCO: 19.2–19.8 wt %, Bayer AG, Leverkusen, Germany), ricinus oil (chemically pure, Beijing Modern Oriental Fine Chemicals Co., Ltd., China), glycerin (chemically pure, Beijing Modern Oriental Technology Development Co., Ltd., China), and triethylamine (chemically pure, Beijing Chemical Works, China) were used to prepare the PU films.

The copolymer latex of styrene, butyl acrylate, and methyl methacrylate (P(St-co-BA-co-MMA) latex) was synthesized by semi-continuous emulsion copolymerization in the presence of functional monomers and emulsifier, synthesized in the Department of Chemical Engineering, Tsinghua University. The latex contained 40 % solid contents and the latex microspheres had an average diameter of 80 nm. The other chemicals were adipic acid dihydrazide (ADH, chemically pure, Beijing J&K Scientific Ltd., China), ethanol (chemically pure, Beijing Modern Oriental Fine Chemicals Co., Ltd., China), urea (chemically pure, Beijing Modern Oriental Fine Chemicals Co., Ltd., China), and deionized water.

The film structure was characterized by a high-resolution scanning electron microscope (SEM, JSM7401, JEOL, Japan). A high-precision scale (BT25S, 0.01 mg, Sartorius AG, Goettingen, Germany) was used to measure the film mass. The concentration of the urea solution was determined by a UV-Vis spectrophotometer (TU-1900, Beijing Purkinje General Instrument Co., Ltd., China). An electronic universal testing machine (AGS-100A, Shimadzu Corporation, Japan) was applied to measure the tensile properties of the film. The degradation of the cross-linking agent was assessed by means of a total organic carbon analyzer (TOC-VCPH, Shimadzu, Japan). A thermogravimetric (TG) analyzer (TGA/DSC 1/1100, Mettler-Toledo International Inc., Switzerland) helped to accomplish the TGA of the irradiated latex.

2.2 Film Preparation

2.2.1 Preparation of Polyolefin Films

An amount of 3 g of PE or PP particles was added into 80 mL of xylene and heated until boiling in a round-bottom flask to dissolve the PE or PP. The solution was coated onto a

25×25 cm² glass sheet wrapped with adhesive tape. The film thickness of 40–50 μm was controlled by scraping the tape at a fixed thickness with a glass bar. The glass sheet was dried at 80 °C for 1 h [24, 25]. Then, the polyolefin film was obtained from the sheet.

2.2.2 Preparation of PU Films

A mixture of 5.2 g ricinus oil, 0.8 g glycerin, 0.2 g triethylamine, and either 4.6 g HDI or 3.0 g MDI was prepared and then coated onto a 25×25 cm² Teflon plate wrapped with adhesive tape. The film thickness of 40–50 μm was controlled by scraping the tape at a fixed thickness with a glass bar. The Teflon plate was dried at 90 °C for 2 h [26, 27]. Finally, the PU film was obtained from the plate.

2.2.3 Preparation of P(St-co-BA-co-MMA) Latex Films

An amount of 10 g P(St-co-BA-co-MMA) latex with 30 % solid content was coated onto a 25×25 cm² glass sheet wrapped with adhesive tape. The film thickness of 40–50 μm was controlled by scraping the tape at a fixed thickness with a glass bar. The glass sheet was dried at 80 °C for 30 min and then heated at 120 °C for 2 h [28]. Then, the P(St-co-BA-co-MMA) film was obtained from the sheet.

The three films, i.e., the film dehydrated at room temperature, the film dehydrated at 80 °C for 30 min, and the film heated at 120 °C for 2 h, were characterized by SEM to analyze the film formation process.

2.3 Measurement of the Film Permeability Coefficient

The film permeability coefficient was measured using a U-shaped tube apparatus, as shown in Fig. S1 in the Supporting Information [29]. A film with a diameter of 40 mm was fixed in the central connector of the U-shaped tubes. The left part of the U-shaped tube was filled with urea-saturated solution and the right part with deionized water. The initial heights of the solutions in both sides of the tube were maintained at the same level. After time Δt ¹⁾, i.e., 48 h, the solution in the right tube was removed to measure the volume and urea concentration, from which the penetration amount of urea, Δm , was calculated.

The urea concentration was measured with a UV-Vis spectrophotometer at 430 nm wavelength [28]. As the permeability coefficient was usually very low for a dense film, the urea concentration (C_w) of the solution in the right tube was very low. The concentration difference across the film was $\Delta C = C_s - C_w \approx C_s$, in which C_s is the urea-saturated concentration. From Fick's first law, the permeability coefficient P of the plane film was calculated by Eq. (1). A repeated measurement

1) List of symbols at the end of the paper.

was conducted and the average of the two measurement values was taken.

$$J = P \frac{\Delta C}{\delta} = \frac{\Delta m}{\Delta t A} \rightarrow P = \frac{\delta \Delta m / \Delta t}{C_s A} \quad (1)$$

where J is the permeation flux, δ is the film thickness measured using a micrometer, and A is the film permeation area.

2.4 Evaluation of Photodegradation

2.4.1 Film Photodegradation

To investigate the film photodegradation performance of polymer materials, an experimental apparatus was designed to examine the film degradation (Fig. S2). The $2 \times 8 \text{ cm}^2$ films were immersed in water in an open box to simulate the water-containing environment of soil, and irradiated under UV light. An aluminum box was used for excellent heat transfer and placed in a thermostatic bath to maintain a constant temperature of 25°C . Four low-pressure mercury lamps (Phillips, 8 W) with a dominant wavelength of 254 nm were set in parallel as the UV light source. The distance from the lamps to the film was 30 mm and the power density of the light was measured as 3.5 mW cm^{-2} . The water in the box was changed after each sampling of every 24 h.

After the film was dried at 80°C for 30 min, after which time the film mass no longer changed, the film was weighed precisely. The mass loss of the film during irradiation was used to characterize the degradation. As a reference, each film was treated and measured under the same conditions without UV irradiation.

To examine the possible residue released from the P(St-co-BA-co-MMA) latex film in water due to degradation, the water in the box was sampled for examination after the film was irradiated for 24 h. The water sample was dropped onto a conductive silicon block and dehydrated in a vacuum drying oven at room temperature. The residue on the silicon surface was observed by SEM.

2.4.2 Cross-Linker Photodegradation

Adipic acid dihydrazide (ADH) served as the cross-linker in P(St-co-BA-co-MMA) latex for cross-linking the microspheres after the latex was dehydrated. To investigate the photodegradation of the cross-linker, a 100 mg L^{-1} ADH solution was irradiated for 1, 2, 3, 4, 5, and 6 h. To examine the generation of carbon-containing gas in the photodegradation of the cross-linker, the total organic carbon (TOC) of the irradiated solution was measured with a TOC analyzer. The oven temperature of the TOC analyzer was set at 680°C .

2.4.3 Microsphere Photodegradation of P(St-co-BA-co-MMA) Latex

To check the degradation of latex microspheres under UV light, a circular groove of Perspex was designed with 25 mm

diameter and $600 \mu\text{m}$ depth. The latex was diluted to 0.5 % solids content for sufficient dispersal. The groove was filled with latex and covered using a thin quartz plate to prevent water evaporation. The latex was irradiated under UV light at 25°C for 10, 20, 30, 40, and 50 h. The size and morphology of the microspheres before and after irradiation were characterized by SEM.

2.5 Mechanical Properties of the P(St-co-BA-co-MMA) Film

The tensile strength of the P(St-co-BA-co-MMA) film after different times of UV light irradiation (0, 72, 144, 216, 288, 360, and 432 h) was investigated using the apparatus shown in Fig. S2. The irradiated films were dried at 80°C for 30 min and were cut into a $1 \times 5 \text{ cm}^2$ strip. The tensile strength of the strip was measured by means of the electronic universal testing machine. The single tensile mode was applied and the tensile rate was set at 10 mm min^{-1} .

The latex with 30 % solid content was irradiated under UV light for different times (0, 24, 48, 72, 96, 120, 144, 168, and 192 h). Then, the film was prepared using irradiated latex and cut into a $1 \times 5 \text{ cm}^2$ strip. The tensile strength of the strip was measured as above.

3 Results and Discussion

3.1 Film Permeability Coefficient

The permeability of urea through a polymer film is affected by several factors, including the film hydrophobicity, film structure, its mechanical strength in the release process, etc. Films with low permeability coefficients can control the nutrient release from a coated fertilizer at a low rate and with high efficiency, with less consumption of coating materials, i.e., a lower cost.

To examine the film permeability of polyolefin, PU, and P(St-co-BA-co-MMA), the permeability coefficients of the films with controlled thicknesses of $40\text{--}50 \mu\text{m}$ were measured as listed in Tab. 1. It was found that among the three types of coating materials, the polyolefin film had the lowest permeability coefficient for urea, followed by P(St-co-BA-co-MMA) and then PU. The low permeability of the polyolefin film was attributed to its high hydrophobicity, while the high permeability

Table 1. Permeability coefficient of urea in different materials.

Material	Film thickness [μm]	Permeability coefficient [$10^{-15} \text{ m}^2 \text{ s}^{-1}$]
Polyolefin	PE 42	1.20
	PP 45	1.80
Polyurethane	PU-HDI 47	7.20
	PU-MDI 49	4.60
P(St-co-BA-co-MMA)	45	2.50

of PU was ascribed to its nonuniform structure caused by insufficient micromixtures and condensation reactions of the two dominant reactants during the film formation process. The P(St-co-BA-co-MMA) film was highly cross-linked and had a dense structure but low hydrophobicity.

The release duration of the controlled-release fertilizer is defined as the time at which 80 % of the nutrients has been released. Shaviv et al. [30] proposed a prediction model with the assumption that the volume of the polymer-coated fertilizer particles do not change. Using this model, the release duration of a 30 μm thick film is longer than 70 days when the film permeability coefficient is $5 \times 10^{-15} \text{ m}^2 \text{ s}^{-1}$ for a urea particle diameter of 3.0 mm. This indicates that the film with a permeability coefficient of less than $5 \times 10^{-15} \text{ m}^2 \text{ s}^{-1}$ can meet the controlled-release requirements of coated urea [31]. This film thickness corresponds to an amount of less than 5 % coating materials by mass, the cost of which is acceptable.

3.2 Photodegradation of the Coating Materials

The mass loss of the PE, PP, HDI-based PU, MDI-based PU, and P(St-co-BA-co-MMA) films changed with the irradiation time under UV light (Fig. 1). It can be seen that all mass loss of the films increased linearly with the irradiation time. However, the PE and PP films exhibited only a little mass loss after irradiation, with mass loss rates per unit area of 1.9 and $8.0 \text{ mg m}^{-2} \text{ h}^{-1}$, respectively. The HDI-based and MDI-based PU films had low mass loss rates per unit area of 10.7 and $14.6 \text{ mg m}^{-2} \text{ h}^{-1}$, respectively. By contrast, the P(St-co-BA-co-MMA) film had the highest mass loss rate per unit area of $61.7 \text{ mg m}^{-2} \text{ h}^{-1}$.

A higher mass loss rate means a higher photodegradation rate. The thicker film labeled as P(St-co-BA-co-MMA)-thicker had with $60.7 \text{ mg m}^{-2} \text{ h}^{-1}$ about the same mass loss rate as P(St-co-BA-co-MMA) with $61.7 \text{ mg m}^{-2} \text{ h}^{-1}$, which indicated that the degradation mass depended on the surface area and was in direct proportion to the power of the irradiating light.

The structures of the five films before and after UV light irradiation were examined using high-resolution SEM and are shown in Fig. S3. Compared with the other four polymer films, the surface morphology of the P(St-co-BA-co-MMA) film changed significantly after degradation. The dense and smooth film surface became porous and rough after degradation. This considerable change of the surface morphology was consistent with the high mass loss, suggesting a different photodegradation mechanism in this film compared to the other films.

The cross-sectional morphology of the P(St-co-BA-co-MMA) film before and after photodegradation is illustrated in Fig. 2. Corresponding to the E2 image in Fig. S3, the surface layer of the P(St-co-BA-co-MMA) film was porous and rough, with a thickness of approximately 1–3 μm and hole sizes of approximately 100–300 nm. The holes were presumed to have formed by generation of gas during the degradation process. These holes loosened the film structure and made it more susceptible to erosion.

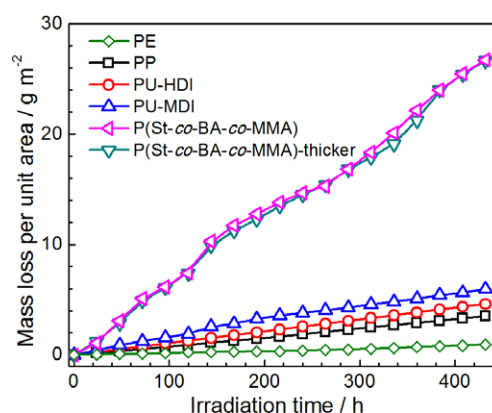


Figure 1. Film mass loss of different coating materials vs. time under UV irradiation. PE, PP, PU-HDI, PU-MDI, P(St-co-BA-co-MMA): 40–50 μm ; P(St-co-BA-co-MMA)-thicker: 80 μm .

A significant change of the film thickness was observed before and after degradation. As displayed in Fig. 3, the film thickness decreased from 52 μm to 25 μm after the P(St-co-BA-co-MMA) film was irradiated for 432 h. The reduction in thickness of 27 μm observed by SEM agreed well with the 26.7 μm decrease calculated using the mass loss per unit area (26.7 g m^{-2}) from Fig. 1 given a material density of 1 g mL^{-1} . This agreement confirmed that the mass loss due to photodegradation occurred mainly on the film surface.

3.3 Photodegradation Process of the P(St-co-BA-co-MMA) Latex Film

3.3.1 Photodegradation of the Cross-Link Chain in the Latex Film

In the synthesis of the P(St-co-BA-co-MMA) latex, adipic acid dihydrazide (ADH) was used as the cross-linker. To avoid the cross-linking of microspheres in the latex, the carboxyl on the microsphere surface was alkalized by adding ammonium hydroxide and converted to carboxylic acid ammonium, which had no catalytic effect on the cross-linking. When the latex was dehydrated, carboxylic acid ammonium was converted back to carboxyl, with a catalytic effect. The carbonyl on the surface of the latex microsphere reacted with ADH under the catalysis of

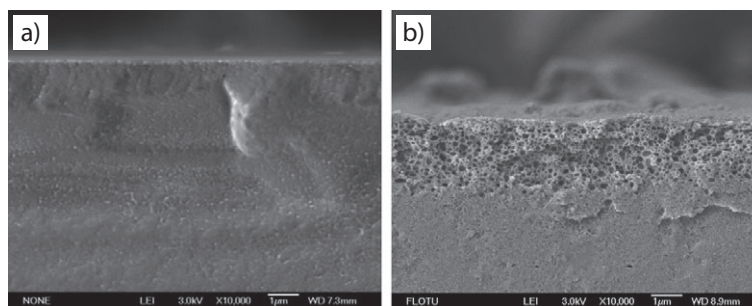


Figure 2. Cross section of the P(St-co-BA-co-MMA) latex film structure (a) before and (b) after UV irradiation for 432 h.

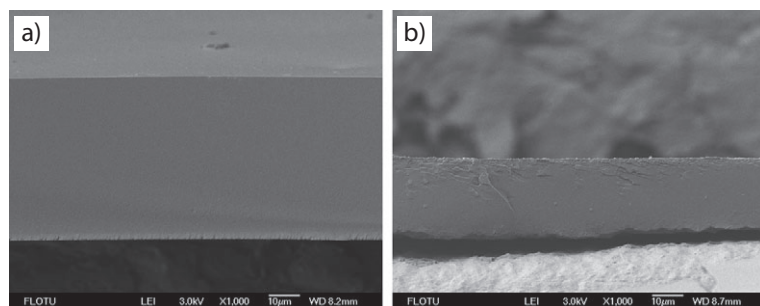


Figure 3. Change in film thickness (a) before (52 μm) and (b) after UV irradiation (25 μm) for 432 h.

carboxyl [32, 33], resulting in cross-linking of the latex microspheres. The cross-linking reaction occurs according to Scheme 1.

During the formation of the P(St-co-BA-co-MMA) latex film, the latex was dehydrated and the microspheres were packed together (Fig. 4 a). When the temperature increased, the microspheres fused with each other and formed an initial film (Fig. 4 b). As the temperature was further increased, the film became uniform and continuous (Fig. 4 c). The cross-linking among the microspheres enhanced the mechanical properties of the latex film. However, though the cross-linker connected the microspheres together under the catalytic effect of carboxyl, the interfaces among those microspheres were not eliminated.

ADH has an active $-\text{CONN}-$ group, which is easily activated under UV light; the $\text{C}-\text{N}$ bond is easily photocleaved [34, 35], leading to the susceptibility of ADH to degradation into smaller molecules. To verify the reaction, the ADH solution of 100 mg L^{-1} was irradiated for different times and the TOC in the solution was measured (Tab. 2). The TOC in the solution decreased significantly from 39.50 to 26.90 mg L^{-1} after 24 h irradiation. This indicated that the cross-linker decomposed and that carbon-containing gas was generated and escaped, leading to the decrease in TOC in the solution. For film degradation, the cross-link chain formed by ADH between the surfaces of the microspheres was broken through the photocleavage of the weak $\text{C}-\text{N}$ bond of the $-\text{CONN}-$ group, and gas containing carbon was generated. This confirmed that the generation of carbon-containing gas due to ADH degradation formed the porous surface displayed in Fig. 2 b.

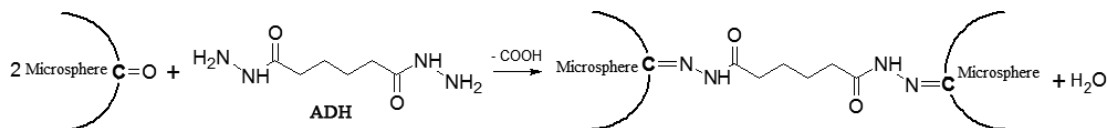
Table 2. TOC in ADH solution after UV irradiation.

Irradiation time [h]	0	4	8	12	16	20	24
TOC of solution [mg L^{-1}]	39.50	37.37	35.22	33.33	30.74	28.65	26.90

3.3.2 Cross-Linking in the Microsphere under UV Irradiation

The microspheres in the diluted latex containing 0.5% solids were irradiated for different times and the morphology was examined (Fig. 5). Size and morphology did not change with the irradiation time, and it was inferred that the mass loss of the P(St-co-BA-co-MMA) film shown in Fig. 1 did not result from the breaking of the polymer microspheres. However, the pH of the latex suspension changed from alkaline (pH 9) to acidic (pH 4) after irradiation, indicating changes in the microsphere surfaces. In addition, the irradiated latex microspheres did not easily form films, indicating that the cross-linking between the microspheres was weakened and the microspheres did not easily fuse.

The TG analysis of the prepared films using the latex irradiated for different times is given in Tab. 3. Compared with the film formed from non-irradiated latex, the weight loss peak and heat flow peak (endothermic) of the film formed from latex irradiated for 144 h increased by 7.9°C and 5.4°C , respec-



Scheme 1. Cross-linking reaction of the latex microspheres.

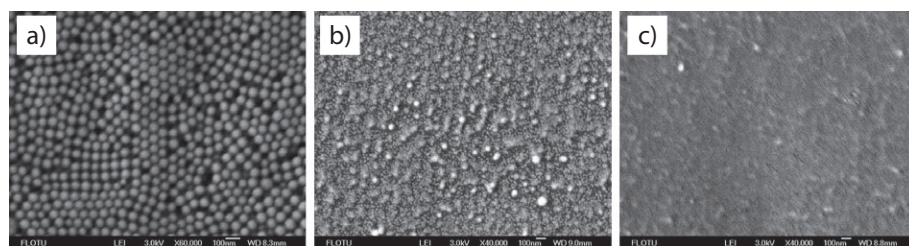


Figure 4. P(St-co-BA-co-MMA) latex film formation process. (a) After dehydration at 25°C ; (b) after drying at 80°C for 30 min; (c) after heating at 120°C for 2 h.

tively. This result indicated that the cross-linking degree of the polymer chains in the microspheres was raised upon irradiation.

The $-\text{CH}-$ group in the polymer chain is active and is easily stimulated by UV irradiation to form radicals that react with other $-\text{CH}-$ groups (Scheme 2). As a result, the polymer chains inside the microspheres were further cross-linked

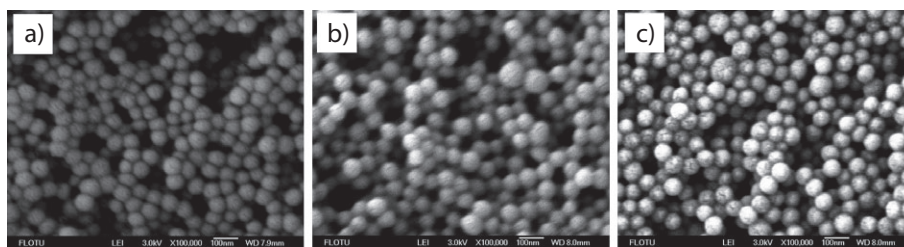


Figure 5. Morphology of microspheres after UV irradiation. Irradiation time: (a) 0 h; (b) 20 h; (c) 50 h.

Table 3. Thermogravimetric analysis of the film formed from irradiated latex.

Irradiation time [h]	0	48	96	144
Weight loss peak [°C]	419.4	422.0	425.9	427.3
Heat flow peak (endothermic) [°C]	423.9	425.5	427.9	429.3

[36, 37]. This resulted in an increased hardness and density of the polymers inside the microspheres. A higher temperature was needed to soften and melt the microspheres.

3.3.3 Microsphere Release from the Film

In the degradation process of the P(St-co-BA-co-MMA) latex film, the residue in the water was sampled and examined by SEM. A large amount of latex microspheres was observed in the water (Fig. 6a), and on the surface of the irradiated film (Fig. 6b). This suggests that the release of microspheres from the film resulted in a great mass loss of the P(St-co-BA-co-MMA) film after irradiation. When the latex film is

photodegraded into microspheres, they have little influence on the moisture level, nutrient delivery, structural properties of the soil, and permeability of molecules or ions into the soil.

3.4 Effects of UV Irradiation on the Mechanical Properties of the P(St-co-BA-co-MMA) Film

Changes in the tensile strength of the P(St-co-BA-co-MMA) films with the time of UV irradiation were measured (Fig. 7). The tensile strength of the film decreased significantly with the irradiation time, with a 77 % reduction after 360 h, for two reasons: the breaking of the cross-link chains weakened the connection between the microspheres, and the cross-linking inside the microspheres led in the increased hardness and density of the microspheres, resulting in a decrease in the film tenacity.

The tensile strength of the film formed from latex irradiated for different times was also measured, as indicated in Fig. 7. For the latex that was irradiated for 144 h under UV light, the tensile strength of the film decreased significantly by 50 %. For longer irradiation times, e.g., 192 h, the latex began to coagulate and failed to form a film because the cross-linking inside the microspheres increased and the microspheres became resistant to fusion, as previously discussed.

Fig. 7 demonstrates that for both the irradiated film and the film formed from irradiated latex, the relationship between the change in tensile strength and the time of UV irradiation was nearly linear, and the average rates of decrease were 37 and 58 kPa h⁻¹, respectively. For the irradiated film, the UV light mainly irradiated the surface of the film due to the attenuation across the film [38], leading to a lower rate of decrease in the tensile strength. For the film formed from irradiated latex, the cross-linker in the latex was broken, and the film formed by the denser and harder microspheres had a weaker tensile strength, leading to a higher rate of reduction.

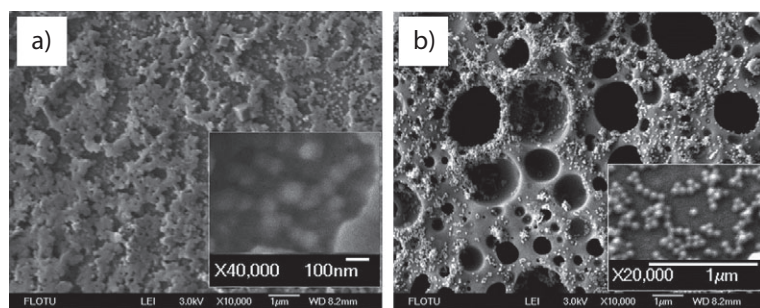
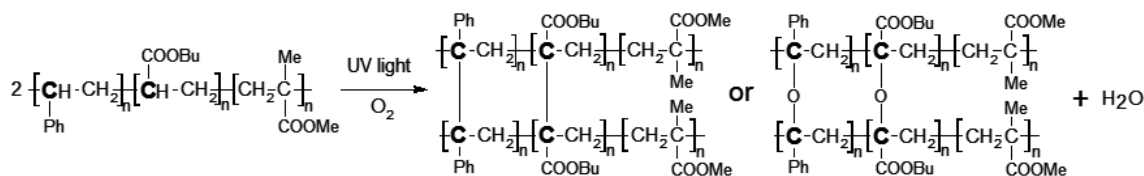


Figure 6. Microspheres released during the film degradation process. (a) In water; (b) on the film surface.



Scheme 2. Aging reaction in $-\text{CH}-$ groups under UV irradiation.

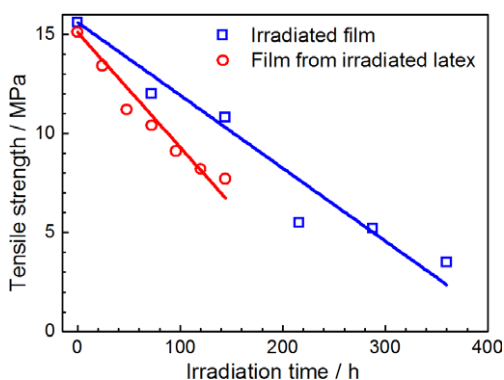


Figure 7. Tensile strength of the irradiated film and the film formed from irradiated latex vs. the time under UV irradiation.

3.5 Photodegradation Mechanism of the Latex Film

The P(St-co-BA-co-MMA) latex film was formed by dehydration of the latex coupled with fusion and cross-linking of the microspheres. A dense and continuous film with low permeability can be obtained when the process is well-controlled. The characteristic of the film is that the interface of the microspheres in the film still exists (Fig. 8 a).

Under UV irradiation, the cross-link chains at the interface of the microspheres broke, producing carbon-containing gas and forming holes in the surface layer of the film. This breaking of the cross-link chains destroyed the connections between the microspheres, leading to an easy release of the microspheres from the film surface (Fig. 8 b). In addition, the cross-linking of the polymer chains within the microspheres was enhanced due to the photo-oxidative aging reaction of the $-CH-$ groups under UV light stimulation. This resulted in an increased density and hardness of the microspheres and a weakened tenacity of the latex film. Thus, the film mass was lost, the film thickness decreased, and the tensile strength of the film decreased with longer UV irradiation times.

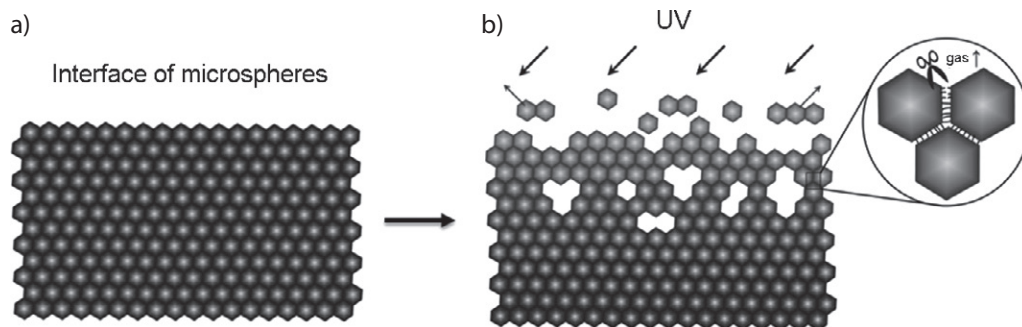


Figure 8. Photodegradation of the polymer latex film under UV irradiation. (a) Latex film; (b) photodegradation.

4 Conclusions

The most commonly used coating materials for producing controlled-release fertilizers, i.e., polyolefin, PU and P(St-co-BA-co-MMA) latex, were employed to prepare films with excellent controlled-release properties. The P(St-co-BA-co-MMA) latex film was degraded at the highest rate under UV irradiation, while the polyolefin and PU films showed little degradation. The surface of the P(St-co-BA-co-MMA) latex film became porous under UV irradiation. The mass loss of the film per unit area reached 26.7 g m^{-2} and the film thickness was reduced by $27 \mu\text{m}$ after 432 h of irradiation. The tensile strength of the polymer latex film decreased by 77 % after 360 h of irradiation.

A novel degradation mechanism of the P(St-co-BA-co-MMA) latex film was confirmed. Under UV irradiation, the cross-link chains were degraded and the connections between the microspheres were destroyed. The photo-oxidative aging reaction occurred in the polymer chains in microspheres in the presence of a tertiary carbon atom ($-CH-$), increasing the degree of cross-linking, resulting in the easy release of microspheres from the film surface and leading to mass loss, reduced thickness, and decreased tensile strength of the film. The specific mechanism by which the film is significantly photo-degraded, the advantages of its excellent controlled-release properties, and its environmentally friendly coating process prove that P(St-co-BA-co-MMA) latex is a promising coating material for controlled-release fertilizers.

Acknowledgment

The authors wish to express their appreciation for the financial support of this study by the National Natural Science Foundation of China (NSFC No. 20876085).

The authors have declared no conflict of interest.

Symbols used

A	$[\text{m}^2]$	permeation area of the film
ΔC	$[\text{g L}^{-1}]$	concentration difference across the film

C_s	$[g L^{-1}]$	saturated concentration of urea solution
C_w	$[g L^{-1}]$	urea concentration in the water tube
J	$[g m^{-2} s^{-1}]$	permeation flux
Δm	$[g]$	penetration amount of urea through the film
P	$[m^2 s^{-1}]$	permeability coefficient of the film
Δt	$[s]$	time interval in measurement

Greek letter

δ	$[m]$	film thickness
----------	-------	----------------

Abbreviations

ADH	adipic acid dihydrazide
HDI	hexamethylene diisocyanate
MDI	diphenyl methane diisocyanate
PE	polyethylene
PP	polypropylene
P(St-co-BA-co-MMA)	copolymer of styrene, butyl acrylate, methyl methacrylate
PU	polyurethane
TOC	total organic carbon
UV	ultraviolet

References

- [1] B. S. Ko, Y. S. Cho, H. K. Rhee, *Ind. Eng. Chem. Res.* **1996**, *35* (1), 250–257. DOI: 10.1021/ie950162h
- [2] K. R. M. Ibrahim, F. E. Babadi, R. Yunus, *Particuology* **2014**, *17*, 165–172. DOI: 10.1016/j.partic.2014.03.009
- [3] D. Davidson, F. X. Gu, *J. Agric. Food Chem.* **2012**, *60* (4), 870–876. DOI: 10.1021/jf204092h
- [4] Y. C. Yang, M. Zhang, Y. Li, X. H. Fan, Y. Q. Geng, *J. Agric. Food Chem.* **2012**, *60* (45), 11229–11237. DOI: 10.1021/jf302813g
- [5] B. Azeem, K. KuShaari, Z. B. Man, A. Basit, T. H. Thanh, *J. Controlled Release* **2014**, *181*, 11–21. DOI: 10.1016/j.jconrel.2014.02.020
- [6] Y. Yang, Z. Tong, Y. Geng, Y. Li, M. Zhang, *J. Agric. Food Chem.* **2013**, *61* (34), 8166–8174. DOI: 10.1021/jf402519t
- [7] R. Lan, Y. H. Liu, G. D. Wang, T. J. Wang, C. Y. Kan, Y. Jin, *Particuology* **2011**, *9* (5), 510–516. DOI: 10.1016/j.partic.2011.01.004
- [8] M. Tzika, S. Alexandridou, C. Kiparissides, *Powder Technol.* **2003**, *132* (1), 16–24. DOI: 10.1016/s0032-5910(02)00345-5
- [9] C. Zhao, Y. Shen, C. Du, J. Zhou, H. Wang, X. Chen, *Ind. Eng. Chem. Res.* **2010**, *49* (20), 9644–9647. DOI: 10.1021/ie101239m
- [10] H. Dong, T. Liu, Z. Han, Q. Sun, R. Li, *J. Environ. Biol.* **2015**, *36* (3), 677–684.
- [11] H. Xie, Y. Li, S. Yang, J. Wang, X. Wu, Z. Wu, *J. Agro-Environ. Sci.* **2007**, *SI*, 153–156. DOI: 10.3321/j.issn:1672-2043.2007.z1.034
- [12] I. Jakubowicz, *Polym. Degrad. Stab.* **2003**, *80* (1), 39–43. DOI: 10.1016/s0141(02)00380-4
- [13] F. Carrasco, P. Pages, J. Gamez-Perez, O. O. Santana, M. L. Maspoch, *Polym. Degrad. Stab.* **2010**, *95* (2), 116–125. DOI: 10.1016/j.polymdegradstab.2009.11.045
- [14] S. Inkinen, M. Hakkarainen, A. C. Albertsson, A. Sodergard, *Biomacromolecules* **2011**, *12* (3), 523–532. DOI: 10.1021/bm101302t
- [15] V. K. Konaganti, G. Madras, *Ind. Eng. Chem. Res.* **2009**, *48* (4), 1712–1718. DOI: 10.1021/ie801646y
- [16] A. Marimuthu, G. Madras, *Ind. Eng. Chem. Res.* **2008**, *47* (7), 2182–2190. DOI: 10.1021/ie0712939
- [17] L. C. K. Liao, M. T. Tung, *Ind. Eng. Chem. Res.* **2006**, *45* (7), 2199–2205. DOI: 10.1021/ie0511130
- [18] X. Zhao, Z. Li, Y. Chen, L. Shi, Y. Zhu, *J. Mol. Catal. A: Chem.* **2007**, *268* (1–2), 101–106. DOI: 10.1016/j.molcata.2006.12.012
- [19] G. Pritchard, *Plastics Additives*, Chapman & Hall, London **1998**.
- [20] M. Tolinski, *Additives for Polyolefins: Getting the most out of Polypropylene, Polyethylene and TPO*, William Andrew, Waltham **2009**.
- [21] M. D. Millan, J. Locklin, T. Fulghum, A. Baba, R. C. Advincula, *Polymer* **2005**, *46* (15), 5556–5568. DOI: 10.1016/j.polymer.2005.05.050
- [22] P. Gijsman, G. Meijers, G. Vitarelli, *Polym. Degrad. Stab.* **1999**, *65* (3), 433–441. DOI: 10.1016/s0141-3910(99)00033-6
- [23] C. Zhang, N. Waksanski, V. M. Wheeler, E. Pan, R. E. Larsen, *Int. J. Eng. Sci.* **2015**, *94*, 1–22. DOI: 10.1016/j.ijengsci.2015.04.006
- [24] L. Wan, X. Zhang, H. Xu, *China Patent 101362663A*, **2008**.
- [25] J. Gao, J. Li, R. You, M. Zhu, X. Liu, *China Patent 103449939A*, **2013**.
- [26] H. Liu, X. Fan, *Mod. Chem. Ind.* **2014**, *10*, 109–111.
- [27] S. Hu, S. Tao, F. Zhang, X. Ren, Y. Cao, R. Jiang, *China Patent 101323545*, **2010**.
- [28] G. Wang, *Master Thesis*, Tsinghua University, Beijing **2013**.
- [29] R. Lan, G. D. Wang, L. Yang, T. J. Wang, C. Y. Kan, Y. Jin, *Chem. Eng. Technol.* **2013**, *36* (2), 347–354. DOI: 10.1002/ceat.201200459
- [30] A. Shaviv, S. Raban, E. Zaidel, *Environ. Sci. Technol.* **2003**, *37* (10), 2251–2256. DOI: 10.1021/es011462v
- [31] A. Shaviv, *Adv. Agron.* **2001**, *71*, 1–49. DOI: 10.1016/s0065-2113(01)71011-5
- [32] B. Thongnuanchan, R. Ninjan, A. Kaesaman, C. Nakason, *Polym. Bull.* **2015**, *72* (1), 135–155. DOI: 10.1007/s00289-014-1264-5
- [33] P. Pi, W. Wang, X. Wen, S. Xu, J. Cheng, *Prog. Org. Coat.* **2015**, *81*, 66–71. DOI: 10.1016/j.porgcoat.2014.12.006
- [34] M. Mashima, F. Ikeda, *Chem. Lett.* **1972**, *3*, 209–214. DOI: 10.1246/cl.1972.209
- [35] K. Waki, J. C. Zhao, S. Horikoshi, N. Watanabe, H. Hidaka, *Chemosphere* **2000**, *41* (3), 337–343. DOI: 10.1016/s0045-6535(99)00500-7
- [36] B. Gewert, M. M. Plassmann, M. MacLeod, *Environ. Sci. Processes Impacts* **2015**, *17* (9), 1513–1521. DOI: 10.1039/c5em00207a
- [37] E. Yousif, R. Haddad, *SpringerPlus* **2013**, *2*, 1–32. DOI: 10.1186/2193-1801-2-398
- [38] B. R. Anderson, M. G. Kuzyk, *Opt. Mater.* **2014**, *36* (7), 1227–1231. DOI: 10.1016/j.optmat.2014.03.004